



Intensification of Low-Temperature Drying of Mushroom by Means of Power Ultrasound: Effects on Drying Kinetics and Quality Parameters

Francisca Vallespir¹ · Laura Crescenzo² · Óscar Rodríguez¹ · Francesco Marra² · Susana Simal¹

Received: 30 November 2018 / Accepted: 5 March 2019 / Published online: 15 March 2019
© Springer Science+Business Media, LLC, part of Springer Nature 2019

Abstract

The aim of this study was to assess the effects of ultrasonic assistance on low-temperature drying of mushroom. For this purpose, mushroom caps slices drying kinetics at 5, 10, and 15 °C without and with ultrasound application (at 20.5 kW/m³) were analyzed, together with the dried product microstructure and some quality parameters (ergosterol and total polyphenol contents, antioxidant activity, color, hydration properties, and fat adsorption capacity). Ultrasound application promoted drying time reductions of 41% at 5 °C, 57% at 10 °C, and 66% at 15 °C, compared with drying without ultrasound. After drying at each temperature, mushroom microstructure presented remarkable tissue shrinkage. Moreover, when ultrasound was also applied, micro-channels were observed. When drying was carried out with ultrasound application, no significant ($p \geq 0.05$) differences or significantly higher ($p < 0.05$) figures of quality parameters were observed, compared with drying without ultrasound application. Thus, mushroom drying process intensification was achieved by using ultrasound, particularly when drying at 15 °C since drying kinetics was enhanced and significantly ($p < 0.05$) smaller changes in all quality parameters were observed, compared with drying without ultrasound.

Keywords Mushroom · Low-temperature drying · Ultrasound · Microstructure · Quality

Introduction

The white button mushroom (*Agaricus bisporus*) contributes about 40% of the total world production of mushroom. It is the most widely cultivated and consumed mushroom throughout the world (Salehi et al. 2017). For centuries, mushrooms have been widely used as a human food, highly appreciated for their healthy properties. They have proven to be effective as antibacterial, antioxidant, anti-inflammatory, antitumor, and antiviral agents (Wu et al. 2016).

Among the biological active substances present in mushrooms, phenolics have attracted much attention due to their high antioxidant activity (Palacios et al. 2011). Moreover, the edible fungi mushrooms are the most important sources for

vitamin D₂ and its precursor, ergosterol, which exists only in the Fungi kingdom (Guan et al. 2016). An important role in regulation of calcium and phosphorus and mineralization of bones in the human body is played by vitamin D (Guan et al. 2016).

In Asia, functional products based on compounds derived from mushrooms or extracts are very common due to their excellent bioactivity (Reis et al. 2017). The study of the properties of mushroom by-products may give information about how they could be incorporated in functional foods. In fact, according to Ekunseitan et al. (2017), the protein present in mushrooms is in forms that are easily digestible and of better quality than those of many legumes sources such as soybeans and peanut. Thus, according to these authors, when mushroom flour proportion was increased in composite flour of wheat and high quality cassava flours, water retention capacity, and fat adsorption capacity significantly increased (Ekunseitan et al. 2017).

Since they have no cuticle to protect them from water loss and physical or microbial attacks, the shelf life of button mushroom is limited to a few days (Zhang et al. 2016). Therefore, they should be consumed or processed rapidly after

✉ Susana Simal
susana.simal@uib.es

¹ Department of Chemistry, University of the Balearic Islands, Ctra Valldemossa km 7.5, 07122 Palma de Mallorca, Spain

² Dipartimento di Ingegneria Industriale, Università degli Studi di Salerno, Via Giovanni Paolo II 132, 84084 Salerno, Italy

harvesting being the drying process one of the oldest methods of mushroom preservation. However, remarkable losses of mushroom quality characteristics could be promoted by drying. According to Çakmak et al. (2016) and Nölle et al. (2017), mushroom bioactive compound contents such as total polyphenol and ergosterol contents were significantly affected (34 and 36% of loss, respectively) after convective drying process at 50 °C (1.5 m/s) and 40 °C (0.6 m/s), respectively. In addition, browning of mushrooms can be indirectly related to quality deterioration due to enzymatic and/or non-enzymatic activity during processing and especially drying, being color a primary quality criterion to consumers, who prefer mushrooms close to their natural appearance (Nölle et al. 2017). Changes in mushroom appearance might also be related to microstructure changes during drying such as tissue shrinkage and collapse (Giri and Prasad 2007).

Low-temperature drying could better preserve the mushrooms quality attributes as they are very sensitive to temperature (Salehi et al. 2017). However, low-temperature drying is a long time and high energy consuming process. Ultrasound application has been reported to enhance low-temperature drying of different fruits and vegetables due to its mechanical energy and mild thermal effect (Santacatalina et al. 2016a). Alternating expansions and contractions when traveling across a medium are generated by the ultrasonic waves, which have a similar effect to that found in a sponge when it is repeatedly squeezed and released (Santacatalina et al. 2016b).

Thus, drying time reductions between 16% in cod slices drying (at 0 °C and 2 m/s) (Santacatalina et al. 2016b) and 75% in apple cubes drying (at 10 °C and 2 m/s) (Santacatalina et al. 2016a) were observed when ultrasound was applied (at power densities of 20.5 kW/m³ and 30.8 kW/m³, respectively, and 22 kHz of frequency). Drying kinetics enhancement could be properly evaluated by using a diffusion model considering both external and internal resistances as it has been demonstrated in previous low-temperature drying studies (García-Pérez et al. 2012a; Santacatalina et al. 2016c). However, due to the “sponge effect” of ultrasound, greater degradation in apple and cod microstructure was observed when drying was carried out with ultrasound application (Ozuna et al. 2014; Santacatalina et al. 2016a).

According to Reay et al. (2013), process intensification leads to substantially more energy-efficient process technology, but in the case of food industry it might also concern quality preservation. Equal or higher losses of bioactive compounds (total polyphenol content and total flavonoid content) and antioxidant activity were reported after ultrasonically assisted (at a power density of 20.5 kW/m³ and frequency of 22 kHz) drying of apple cubes (8.8 mm side) at low-temperature drying (at temperatures of 0, 5, and 10 °C and air velocity of 1 m/s), in comparison with changes after drying without ultrasound application (Santacatalina et al. 2014, 2016a). Meanwhile, color coordinates (CIELab scale) of cod

slices dried (at temperatures of 0, 10, and 20 °C and air velocity of 2 m/s) with ultrasound application (at a power density of 20.5 kW/m³ and frequency of 22 kHz) presented negligible differences to salted cod dried without ultrasound application (Ozuna et al. 2014; Santacatalina et al. 2016b). Unfortunately, in the literature, there is scarcely any study about mushroom low-temperature drying intensification by using ultrasound application.

Therefore, the main aim of this study was to evaluate the effects of ultrasound application on the low-temperature drying kinetics and quality parameters of mushroom. Therefore, drying kinetics and changes promoted in microstructure, ergosterol and total polyphenol contents, antioxidant activity, color, hydration properties, and fat adsorption capacity after drying without and with ultrasound were evaluated.

Materials and Methods

Sample Processing

Preparation

White button mushrooms (*Agaricus bisporus*) were purchased in a local market in Palma de Mallorca (Spain). Mushrooms with uniform color and size (5 cm of diameter approx.) were selected. The stems were removed and only the caps were used for the experiments. They were washed with tap water and sliced to a thickness of 0.005 m with a sharp knife cutting them vertically and immediately processed to avoid degradation. Blanching pre-treatment with steam of boiling water (at 100 ± 5 °C) during 15 s was applied in order to reduce browning process. After blanching, the excess of water on the surface of the slices was drained with tissue paper. Then, by using the AOAC method No. 934.06 (AOAC 2006), the initial average moisture content (W_0 , kg/kg d.m.) was obtained. Finally, the slices were placed on a stainless-steel load tree, which was hanged into the dryer.

Drying Experiments

Drying experiments were carried out in a convective dryer with air recirculation, air velocity and temperature control, and an ultrasonically activated drying chamber, which was already described by Vallespir et al. (2018). A scheme of the convective drier was also reported by Vallespir et al. (2018). The drying experiments were carried out at the temperatures of 5, 10, and 15 °C in an industrial upright fridge ACRV-125-2 (Coreco, Spain). The air velocity was of 1 m/s and the air relative humidity was of 28 ± 7%. An electrical power of 50 W (20.5 kW/m³) and 22 kHz was applied in the drying experiments with ultrasound application (AIR+US) and no electrical power was applied in the drying experiments

without ultrasound application (AIR). Drying experiments were carried out until an 85% of weight loss with respect to initial weight was achieved. Sample was periodically weighed at selected times. At least, triplicates of each experiment were done.

Shrinkage Correlations

The contraction of the slab shape was considered as both the contraction of the thickness and the contraction of the face area. The thickness and face area shrinkage correlations were experimentally estimated. Slab-shaped mushroom samples ($4.9 \pm 0.2 \times 10^{-3}$ m thickness and $1.44 \pm 0.05 \times 10^{-4}$ m² of face area) were used to determine the change of the sample thickness and area during drying. The samples were dried during the different times: 100, 200, 360, 450, and 600 min at 15 °C and 1 m/s. The shrinkage was measured in five samples at each different drying time. The changes in thickness (Th) were calculated using the dimensions determined by a caliper. The changes in the face area (A) were measured by using an image acquisition system which consisted of a digital camera vertically placed above the sample at a distance of 0.1 m from its upper face. The illumination was achieved with four fluorescent light tubes (power, 35 W; length, 0.30 m; color temperature, 2700 K; light flux, 270 lm). Both the camera and the illumination system were placed in a wooden box whose walls were painted in black to minimize the background light. Four images were acquired for each sample (two of each side) at each time, thus 20 photos of each time were processed. Image managing involved the adjustment of the pictures with Microsoft Office Picture Manager® software (Microsoft, Seattle, USA) (color and shades correction tools) and the area measurement with an algorithm developed by using the Image Acquisition Toolbox of Matlab® software (The Mathworks, Inc., Natick, USA). The area measurements were correlated to the surface of 1 and 2 euros coins, since these objects have official surface values given by “Fábrica Nacional de Moneda y Timbre-Real Casa de la Moneda” (Spanish Government 2018). Also, the moisture content of the samples at each time was obtained by means of the AOAC method No. 934.06 (AOAC 2006).

Modeling

In order to obtain a mathematical model representative of the moisture transport during the drying process, the process was considered to be isothermal and the microscopic mass transfer balance was combined with Fick’s second law. Considering moisture diffusion to be the main transport phenomenon, the governing equation for transient mass transfer by effective diffusion in the considered slab geometry was formulated as (Eq. 1).

$$D_e \frac{\partial^2 W}{\partial x^2} = \frac{\partial W}{\partial t} \quad (1)$$

The constant and effective diffusion coefficient (D_e), representative of the global transport process, might include molecular diffusion, liquid diffusion through the solid pores, vapor diffusion, and all other factors which affect drying characteristics (Rodríguez et al. 2013). As an initial condition, the moisture distribution inside the solid was considered to be uniform at the beginning of the process (Eq. 2). Moisture distribution symmetry (Eq. 3) and the external mass transfer at the solid surface (Eq. 4) were considered as boundary conditions.

$$W_{(x)}|_{t=0} = W_0 \quad (2)$$

$$\frac{\partial W}{\partial x} \Big|_{x=0, t>0} = 0 \quad (3)$$

$$-D_e \rho_{dm} \frac{\partial W}{\partial x} \Big|_{x=L, t>0} = h_m (\varphi_e - \varphi_\infty) \quad (4)$$

The sorption isotherm reported by Iglesias and Chirife (1982), the shrinkage correlations and the psychrometric data were considered to complete the model.

COMSOL Multiphysics® 5.1 software (COMSOL Inc., Sweden) was used to solve the mathematical model, applying the finite elements method. After the mesh independence test, a domain composed of about 54 elements, resulting in about 110 degrees of freedom was used. Matlab 2014a® software (The Mathworks, Inc., Natick, USA) was used to develop the algorithm, by using the “fminsearch” Matlab function, to identify both the effective diffusion (D_e , m²/s) and the external mass transfer (h_m , kg water/m² s) coefficients from each drying curve through the minimization of the objective function: mean relative error between calculated and experimental average moisture content, given by the Eq. 5.

$$MRE (\%) = \frac{100}{n} \sum_{i=1}^n \left| \frac{W_{exp_i} - W_{cal_i}}{W_{exp_i}} \right| \quad (5)$$

Microstructure Observation

According to the methodology described by Eim et al. (2013) with minor modifications, dried mushroom slices at 5, 10, and 15 °C without (AIR) and with ultrasound application (AIR+US) were prepared for the light microscopy observation. Formaldehyde (10%) was used to fix the samples followed by dehydration, embedded in paraffin (60 °C for 3 h) and sectioned by a microtome Finesse 325 (Thermo Shandon, UK) into 4–5-μm sections. The sections were stained with Hematoxylin Eosin (H-E) and Periodic Acid–Schiff (PAS) to

visualize cell walls (Paciulli et al. 2015). In order to obtain the microstructural images, an optical microscope BX41 (Olympus, Japan) and a camera DP71 (Olympus, Japan) at 100 magnifications were used. Six sections of each sample were prepared and 12 micrographs of each sample were obtained, at least.

Bioactive Compounds and Antioxidant Activity Analyses

The samples dried at 5, 10, and 15 °C without (AIR) and with (AIR+US) ultrasound application were analyzed to determine their ergosterol (EC) and total polyphenol (TPC) contents and antioxidant activity (AA).

Ergosterol Content

A simple direct extraction of ergosterol using hexane was used according to the methodology proposed by Shao et al. (2010) with minor modifications. An internal standard (cholecalciferol 1 mg/mL) was used during the extraction of the sample powder. To prepare the mushroom powders, dried samples were pulverized in an A10 grinder (Janke and Kunkel IKA Labortechnik, Germany) and sieved in an FTL-0200 sieve (Filtru, Spain) in order to obtain a particle size powder of 90–180 µm. The mushroom powder of 0.05 g was vortexed with 6 mL of hexane and 0.5 mL of internal standard for 1 min and centrifuged at 4000 rpm for 10 min. The supernatant (hexane phase) was decanted and transferred into a vial. Two more extractions were carried out to the mushroom residue also with 6 mL of hexane. All the hexane extract was dried by using a stream of argon and dissolved in 2 mL of ethanol. Finally, it was filtered through a 0.22-µm PVDF filter before HPLC analysis.

An HPLC system 600 (Waters, USA) equipped with an inline degasser, a quaternary pump Delta 600E (Waters, USA), a thermostatic autosampler 717 plus (Waters, USA), and a photodiode array detector (PDA detector) 2996 (Waters, USA) was used. A Nova-Pak 4 µm C18 column (3.9 × 150 mm) (Waters, USA) was used for the separation. The mobile phase consisted of solvent methanol/water, 80:20 v/v. The injection volume was of 2 µL for the standard and samples and the flowrate was of 1.0 mL/min. Absorbance at 280 nm was used to monitor and quantify ergosterol. A combination of the retention time in HPLC chromatograms and UV spectra was used to tentatively identify ergosterol in mushroom samples. Absorbance measurements were correlated with standard curves of commercial ergosterol (0.05–0.7 mg/mL) together with the internal standard. The results were expressed as µg of ergosterol/g d.m.

Total Polyphenol Content and Antioxidant Activity

According to the methodology described by Heredia and Cisneros-Zevallos (2009) with some modifications, methanol extracts from the mushroom slices were prepared. Twenty milliliters of methanol extraction solvent was added to samples accurately weighed (ca. 0.1 g of dried samples). By using Ultra-Turrax© T25 Digital (IKA, Germany) at 13,000 rpm for 1 min at 4 °C the mixture was homogenized and then the obtained solution was refrigerated overnight. Mixtures were centrifuged at 4000 rpm for 10 min before filtration. The extracts were refrigerated at 4 °C until analysis. At least, four methanol extracts were prepared for each sample.

According to Eim et al. (2013) by means of the Folin-Ciocalteu assay, total polyphenol content (TPC) was determined. By using FRAP, CUPRAC, and ABTS methods according to González-Centeno et al. (2012) the antioxidant activity (AA) was determined. An UV/Vis/NIR spectrophotometer Multiskan Spectrum (Thermo Scientific, Finland) at 25 °C and at 745, 593, 450, and 734 nm was used to carry out the absorbance measurements in TPC, FRAP, CUPRAC, and ABTS methods, respectively. Absorbance values were correlated with standard curves (0–250 mg/L gallic acid for TPC and 0–400 mg/L trolox for AA). The results were expressed as milligram of gallic acid equivalent (GAE)/g d.m. for the TPC, while the AA was expressed as milligram of trolox equivalent (TE)/g d.m.

Color Determinations

Color of mushroom samples dried at 5, 10, and 15° without and with ultrasound application was measured using the sieved powder at a particle size of 90–180 µm. The CIElab color space was used to estimate the color values of mushroom samples. The coordinates were L^* (whiteness or brightness/darkness) a^* (redness/greenness), and b^* (yellowness/blueness). A CM-5 colorimeter (Konica Minolta, Japan) with a D65 illuminant and 2° observer (Urun et al. 2015) was used to carry out the measurements. The browning index (BI) of the dried samples was determined according to the equations proposed by Farokhian et al. (2017) (Eq. 6).

$$\text{BI} = \frac{[100(x-0.31)]}{0.17}, \text{ where } x = \frac{(a^* + 1.75L^*)}{(5.645L^* + a^* - 3.012b^*)} \quad (6)$$

Hydration Properties and Fat Adsorption Capacity

Properties measured in this study included hydration properties, such as swelling (SW) and water retention capacity

(WRC), and fat adsorption capacity (FAC). These properties were determined according to the methodology described by Femenia et al. (2009) with minor modifications. All the properties were measured using dried samples powders (90–180 μm), which preparation was specified above.

Swelling (SW) was determined hydrating approximately 60 mg of sample powder with excess of water (10 mL) during 24 h and measuring the final volume of sample. SW results were expressed as mL/g d.m. Water retention capacity (WRC) was determined hydrating ca. 10 mg of sample powder with water in excess (5 mL) in a 10-mL tube during 24 h. The sample was then centrifuged at 2000 rpm for 20 min, the supernatant was decanted and the sample weight was taken. WRC was expressed as g/g d.m. Finally, fat adsorption capacity (FAC) was determined as the oil adsorption capacity. Samples (ca. 10 mg of powder) were mixed with sunflower oil (5 mL), rested 24 h, centrifuged at 2000 rpm for 20 min, the supernatant was decanted and the sample weight was taken. FAC was expressed as g/g d.m.

Statistical Analyses

Data were averaged from corresponding replicates and reported as average values \pm standard deviations. Analysis of variance (ANOVA) was applied to analyze the effects of both the drying temperature and the ultrasound application during drying on the identified coefficients of the diffusion model, ergosterol and total polyphenol contents, antioxidant activity, color, hydration properties, and fat adsorption capacity. Means were compared by Tukey's test at $\alpha = 0.05$. Statistical analyses were carried out using R: Language and Environment for Statistical Computing (R Core Team, Austria).

Additionally, besides MRE, the percentage of explained variance (Eq. 7) was used to further evaluate the accuracy of the obtained simulation of the drying curves.

$$\text{var} (\%) = \left[1 - \frac{S_{xy}}{S_y} \right] \times 100 \quad (7)$$

Results and Discussion

Drying Kinetics

Initial moisture content of fresh mushroom after blanching was of 11.8 ± 0.8 kg/kg d.m., which was similar to the reported by Zhang et al. (2016) in fresh mushroom (11.5 ± 0.1 kg/kg d.m.). Final moisture content was of 0.95 ± 0.04 kg/kg d.m. after 85% of weight loss. The experimental drying kinetics of mushroom slices at 5, 10, and 15 °C and 1 m/s, without (AIR) and with ultrasound application (AIR+US) (20.5 kW/m^3), are

shown in Fig. 1. No significant differences ($p \geq 0.05$) were observed between drying kinetics at 5 and 10 °C when ultrasound was not applied (5 °C AIR and 10 °C AIR experiments). However, the drying kinetics at 15 °C was significantly shorter ($p < 0.05$) than those at 5 and 10 °C, without using ultrasound. When ultrasound was applied (AIR+US), significantly shorter ($p < 0.05$) drying kinetics than the corresponding kinetics without ultrasound application (AIR) were observed at every temperature used. Thus, drying time needed at 5 °C of air temperature without ultrasound application (AIR) to reach a moisture content of ca. 1 kg/kg d.m. (0.99 ± 0.07 kg/kg d.m.) was of 21 h and, when ultrasound was applied (AIR+US), the drying time was shortened by 41%. In the case of drying at a temperature of 10 °C without ultrasound application (AIR), drying time was of 20 h and it was shortened by 57% with ultrasound application (AIR+US). Finally, 18 h were needed when drying was carried out at 15 °C without ultrasound application (AIR) and when ultrasound was applied (AIR+US), drying time was shortened a 66%, thus only 6 h were needed.

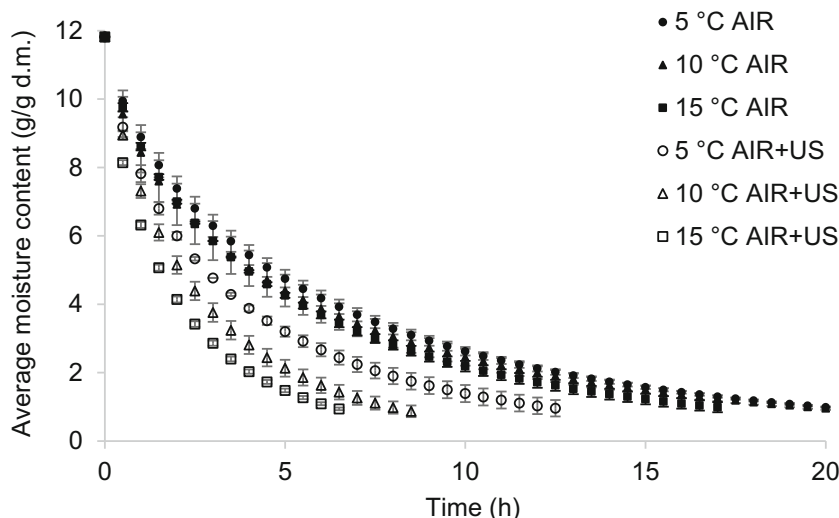
No bibliography of mushroom drying intensification by ultrasound application during drying was found. In other products, similar drying time reductions were observed by Santacatalina et al. (2014) (60%), Ozuna et al. (2014) (36–55%) and Santacatalina et al. (2016c) (44%) in low-temperature drying of apple cubes (at 0, 5, and 10 °C and 2 m/s), cod parallelepipeds (at 0, 10, and 20 °C and 2 m/s), and eggplant cubes (at 10 °C and 4 m/s), respectively, when ultrasound was applied (20.5 kW/m^3).

As the temperature rises, higher drying time reductions were observed when ultrasound was applied (AIR+US experiments) compared with AIR experiments. Similar behavior was observed by Ozuna et al. (2014) and by Santacatalina et al. (2016b) in cod low-temperature drying at 0–10 °C and 0–20 °C, respectively. Thus, these authors observed higher drying time reductions when applying ultrasound at higher temperatures. Moreover, Gamboa-Santos et al. (2014) reported also higher drying time reductions in strawberry hot air drying when the temperature rose from 40 to 50 and to 60 °C, although at 70 °C the drying time reduction was lower than at 50 °C. Santacatalina et al. (2014) and Santacatalina et al. (2016c) reported higher drying time reductions when temperature rose from 0 to 10 °C in low-temperature drying assisted by ultrasound of apple and eggplant, respectively. Therefore, it seems that the range of temperatures tested and the structure of the product may affect the ultrasound effects when temperatures rise.

Shrinkage Correlations

Shrinkage of the sample was monitored during drying of mushroom samples at 15 °C without ultrasound application. Shrinkage was assumed to be constant in the range of

Fig. 1 Mushroom experimental drying kinetics at 5, 10, and 15 °C without (AIR) and with 20.5 kW/m³ and 22 kHz of ultrasound application (AIR+US). Average values ± standard deviations



conditions assayed in this study: 5, 10, and 15 °C without (AIR) and with (AIR+US) ultrasound application since no differences were observed in previous experiments under different temperatures and ultrasound application. Experimental results of thickness (Th) and face area (A) at different moisture contents were fitted to linear regressions obtaining Eq. 8 (thickness) and Eq. 9 (face area).

$$\frac{Th}{Th_0} = 0.325 + 0.689 \frac{W}{W_0} \quad R^2 = 0.985 \quad (8)$$

$$\frac{A}{A_0} = 0.324 + 0.676 \frac{W}{W_0} \quad R^2 = 0.994 \quad (9)$$

Both linear regressions presented high correlation coefficients close to the unit, thus, the linear adjustment was considered satisfactory. The obtained relationships were similar to that found by Gamboa-Santos et al. (2014) in strawberry cubes hot air drying (70 °C) between the characteristic diffusion dimension (L) and moisture ratio (W/W_0). However, different shrinkage correlation figures ($\frac{V}{V_0} = 0.112 + 0.929 \frac{W}{W_0}$) were reported by García-Pérez et al. (2011) in eggplant cubes hot air drying (40 °C). For instance, when the eggplant sample moisture content was reduced by 50%, the volume was reduced by 58%. Meanwhile, in the present study, when kiwifruit samples moisture content was reduced by 50% thickness and the face area were reduced by 67 and 66%, respectively. This fact is probably due to different drying conditions and product structure.

Modeling of Drying Kinetics

Table 1 shows the effective diffusion and external mass transfer coefficients (D_e and h_m) identified by using the proposed model and minimizing the MRE between calculated and experimental average moisture content (Eq. 5). In this table, the

average MRE (%) and the percentage of explained variance (var, %) of the simulation are also shown.

The identified D_e ranged from 2.68 (5 °C) to 3.39×10^{-11} m²/s (15 °C) in AIR experiments, meanwhile in AIR+US experiments this coefficient ranged from 4.71 (5 °C) to 9.62×10^{-11} m²/s (15 °C). These figures were in the range of those observed by Santacatalina et al. (2014) in the low-temperature drying of apple (2 m/s) when drying was carried out without acoustic assistance (from 3.3 at 0 °C to 8.8×10^{-11} m²/s at 10 °C) and when an acoustic power of 20.5 W/m³ was applied (from 8.6 at 0 °C to 22.3×10^{-11} m²/s at 10 °C). Higher effective moisture diffusivity figures were reported by Mihalcea et al. (2016) during the mushroom hot-air drying process at 50, 60, and 70 °C and 0.55 m/s: 1.10 – 2.12×10^{-10} m²/s, due to the higher drying temperature which enhances moisture diffusion.

As it can be observed in Table 1, the higher the drying temperature, the higher the effective diffusion coefficient. Thus, when temperature was increased from 5 to 15 °C, identified effective diffusion coefficient increased by 26 and 104% in AIR and AIR+US experiments, respectively. However, as it was expected from drying kinetics, identified D_e coefficients of AIR experiments at 5 and 10 °C were not significantly different ($p \geq 0.05$).

Ultrasound application also increased identified D_e coefficients by 76% at 5 °C, 135% at 10 °C, and 184% at 15 °C. Therefore, a faster water removal was observed during the drying process as consequence of the acoustic assistance. The mechanical force given by the acoustic waves can create microscopic channels that allow an easier inner water movement without a significant overheating of the material (García-Pérez et al. 2012b). Moreover, as it was expected from the drying kinetics when ultrasound was applied, higher effective diffusion increases were obtained at higher temperatures as it was also observed in cod drying by Ozuna et al. (2014) (at 0,

Table 1 Identified effective diffusion coefficient (D_e) and the external mass transfer coefficient (h_m) together with the MRE and var for each set of mushroom drying experiments without (AIR) and with 20.5 kW/m³ of acoustic assistance (AIR+US) at drying temperatures of 5, 10, and 15 °C. Average values ± standard deviations. Means with different letter for D_e or h_m showed significant differences according to Tukey’s test ($p < 0.05$)

T (°C)	5	10	15
<i>AIR</i>			
$D_e \times 10^{11}$ (m ² /s)	2.68 ± 0.12 <i>e</i>	2.92 ± 0.18 <i>e</i>	3.39 ± 0.09 <i>d</i>
$h_m \times 10^5$ (kg water/m ² s)	4.37 ± 0.19 <i>e</i>	4.54 ± 0.08 <i>e</i>	5.06 ± 0.14 <i>d</i>
MRE (%)	4.3 ± 1.2	1.8 ± 0.8	2.8 ± 1.1
var (%)	99.6 ± 0.3	99.7 ± 0.2	99.9 ± 0.1
<i>AIR+US</i>			
$D_e \times 10^{11}$ (m ² /s)	4.71 ± 0.05 <i>c</i>	6.87 ± 0.23 <i>b</i>	9.62 ± 0.31 <i>a</i>
$h_m \times 10^5$ (kg water/m ² s)	7.04 ± 0.07 <i>c</i>	8.87 ± 0.30 <i>b</i>	13.01 ± 0.42 <i>a</i>
MRE (%)	1.0 ± 1.2	3.4 ± 1.7	3.2 ± 1.2
var (%)	99.9 ± 0.1	99.9 ± 0.1	99.9 ± 0.1

10, and 20 °C) and by Santacatalina et al. (2016b) (at 0 and 10 °C).

Effective diffusion coefficient temperature dependence was correlated to Arrhenius equation (Eq. 10) in AIR and AIR+US experiments obtaining a correlation coefficient of the linear equation close to the unity in both cases (0.97 and 0.99 in AIR and AIR+US experiments, respectively).

$$\ln(D_e) = \ln(D_o) - \frac{E_a}{R(T + 273.15)} \tag{10}$$

The estimated activation energy E_a for AIR and AIR+US experiments were of 15.53 ± 0.04 and 47.4 ± 0.3 kJ/mol, respectively. The acoustic assistance promoted an increase of 206% of this parameter. Thus, as it was observed in the drying kinetics, higher ultrasound application effects were observed at higher drying temperatures.

The identified h_m , presented in Table 1 was also affected by both, the drying temperature and the acoustic assistance. Thus, h_m ranged from 4.37 × 10⁻⁵ kg water/m²·s at 5 °C in drying without ultrasound to 13.01 × 10⁻⁵ kg water/m²·s at 15 °C in acoustically assisted drying. Slightly higher h_m figures were reported in low-temperature drying without ultrasound application of apple (4.3 × 10⁻⁴ kg water/m²·s) at 10 °C and 2 m/s (Santacatalina et al. 2016a) and eggplant (0.8 × 10⁻³ and 1.3 × 10⁻³ kg water/m²·s) at 0 °C and at 10 °C, respectively, and 1 m/s (Santacatalina et al. 2016c), probably due to differences in drying conditions and sample which modify the solid surface moisture transfer.

The rise of the drying temperature from 5 to 15 °C, slightly increased the h_m by 16% in AIR experiments but increased by 85% the h_m in AIR+US experiments. Thus, as it was observed in drying kinetics and D_e coefficient, in AIR+US experiments higher effects of temperature rising are obtained.

The acoustic assistance also increased h_m . The increment in this coefficient was higher at 15 °C (157%), meanwhile at 5 °C the increment was of 61%. Thus, the acoustic assistance induced a decrease of the external resistance to the mass transfer due to the pressure variations at the solid/gas interfaces

and, therefore, the surface moisture evaporation rate increased (Rodríguez et al. 2014). The positive ultrasound effect on h_m was also reported by Santacatalina et al. (2014) and by Santacatalina et al. (2016c) in acoustically assisted (20.5 kW/m³) low-temperature drying at an air velocity of 1 m/s of apple and eggplant, respectively. However, these authors reported lower external mass transfer coefficient increments when ultrasound was applied at higher temperatures and in the present study, the opposite behavior was observed, higher h_m increments were observed as the temperature rises when ultrasound was applied. Similarly, Gamboa-Santos et al. (2014) observed also higher h_m increments when ultrasound was applied in strawberry hot air drying when the temperature rises from 40 to 50 and to 60 °C, although at 70 °C the h_m increment when ultrasound was applied was lower than that at 50 °C.

External mass transfer coefficient temperature dependence was adjusted to a linear regression obtaining a correlation coefficient close to the unity in AIR and AIR+US experiments according to Eq.11 and Eq. 12.

$$\text{AIR } h_m = 3.96(\pm 0.09) \times 10^{-5} + 6.9(\pm 0.2) \times 10^{-7} \cdot T(^{\circ}\text{C}) \quad R^2 = 0.92 \tag{11}$$

$$\text{AIR + US } h_m = 3.68(\pm 0.20) \times 10^{-5} + 6.0(\pm 0.9) \times 10^{-6} \cdot T(^{\circ}\text{C}) \quad R^2 = 0.95 \tag{12}$$

As it can be observed in Eqs. 11 and 12, AIR+US correlation equation presented higher average slope fig. (6.0 × 10⁻⁶ kg water/m² s·°C) than AIR correlation eq. (6.9 × 10⁻⁷ kg water/m² s·°C). Therefore, AIR+US experiments were more affected than AIR experiments by temperature factor, as it was expected from the drying kinetics.

The drying curves were simulated and represented in Fig. 2 by using the proposed model and Eqs. 10–12 together with the estimated D_o and E_a figures. In Fig. 2, the experimental data were represented against the predicted data for all the experiments. The linear regression and the predicted bounds at a

95% confidence were also shown in this figure. From the coefficient of determination (close to the unit, 0.99), the slope and the y-intercept, which were close to the unit (1.01) and zero (-0.027), respectively, it could be concluded that a good agreement between the experimental and the predicted data was found. Moreover, the simulation was mathematically evaluated by using the MRE (%) and var (%) statistics, both also included in Table 1. It could be concluded from Fig. 2 and Table 1 that the drying curves of mushroom dried at 5, 10, and 15 °C without and with acoustic assistance (20.5 kW/m^3) could be satisfactorily simulated by using the proposed model.

In conclusion, the use of the proposed model allowed us the evaluation of the influence of both temperature and ultrasound on the external and the internal mass transfer resistances. From the figures obtained for the diffusion coefficient and the mass transfer coefficient, it could be concluded that the use of acoustic energy contributed to accelerate the drying process not only decreasing the external resistance but also increasing the water mobility inside the food. The mechanical vibration produced by the ultrasound application affected both, the internal resistance to the mass transport by successive compressions and expansions of the material (“sponge effect”), and also the external resistance to the mass transport due to the reduction of the boundary layer which eases the vapor transfer rate from the solid surface to the drying air (Rodríguez et al. 2018). The sum of both effects led to an important increase of the water release rate during the drying process.

Microstructure Observation

Light microscope micrographs of dried samples at 5, 10, and 15 °C without (AIR) and with (AIR+US) 20.5 kW/m^3 of ultrasound application are shown in Fig. 3. As it was reported

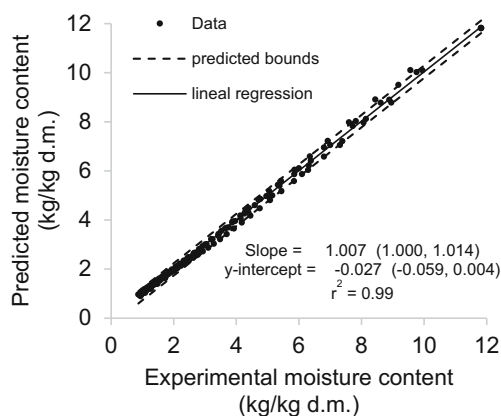


Fig. 2 Predicted vs experimental moisture content, linear regression (slope and y-intercept) and predicted bounds at 95% of confidence of mushroom drying kinetics at 5, 10, and 15 °C without and with 20.5 kW/m^3 and 22 kHz of ultrasound application. Slope and y-intercept 95% of confidence limits are presented in brackets

by Pei et al. (2014) and it could also be observed in this figure, mushroom microstructure presents a large amount of holes in a honeycomb ultra-structure. Mihalcea et al. (2016) described the mushroom microstructure as an ensemble of typical fungal hyphae cells whose mechanical strength is due to chitin. These hyphae cells were observed by Mihalcea et al. (2016) in fresh sample and could also be observed in dried samples in Fig. 3.

After drying without ultrasound application (AIR), the mushroom microstructure observed in Fig. 3 presented tissue shrinkage (s) and collapse in some zones compared with others as it was observed by Giri and Prasad (2007) after mushroom drying at 60 °C and 1.5 m/s. Moreover, according to Mihalcea et al. (2016) during the mushroom drying process at 50, 60, and 70 °C and 0.55 m/s the intercellular spaces between hyphae cells enlarged and became more pronounced. This hollowing out phenomenon, also observed in Fig. 3 (h) (AIR), could be the result of the decreasing hyphae turgidity when the water was lost. So, the tissue lost its capacity to hold the water and shrank (Mihalcea et al. 2016). Furthermore, according to Lombraña et al. (2010) and Mihalcea et al. (2016) when drying mushroom slices at different temperatures (60–80 °C and 50–70 °C, respectively), more pronounced shrinkage and hollowing out phenomena were observed when increasing temperature as it was also observed in Fig. 3 (AIR).

Regarding the ultrasound effects, micro-channels were observed in Fig. 3 (m) (AIR+US) together with convective drying shrinkage (s) when mushroom drying was carried out at 5, 10, and 15 °C with ultrasound application (20.5 kW/m^3). When ultrasound was applied, micro-channels observed in Fig. 3 (AIR+US) in dried samples at 15 °C, were in general, wider than those of dried samples at 5 and 10 °C, which might be related to a higher ultrasound effect and consequent higher drying time reduction mentioned in the “Drying kinetics” section. According to Islam et al. (2014) and Islam et al. (2015), mushroom tissue presented damages to the cells such as twisting or wrinkling due to sponge effect of ultrasound which create micro-channels through the membrane when ultrasound was applied during freezing at -20 °C in a bath with a probe (20 kHz, $0.13\text{--}0.39 \text{ W/cm}^2$) or by direct contact with a chamber (20 kHz, 300 W), respectively. Furthermore, when ultrasound pre-treatment with a probe (40 kHz, 0.44 W/cm^2) was applied before mushroom drying at 60 °C and 0.5 m/s, breakdown of cell walls, decreased intercellular contact and collapse of cell structure were observed by Zhang et al. (2016). No references about ultrasound application on mushroom drying at low-temperature were found but a comparison with other products was done. According to Santacatalina et al. (2016a) and Ozuna et al. (2014), a greater degradation of the structure causing an increase in product porosity and pore diameter that eased the water movement in the matrix during drying was observed when applying ultrasound (25–75 W and 20.5 kW/m^3 , respectively) during the low-temperature drying of apple (at 10 °C and -10 °C and

2 m/s) and salted cod (at -10 , 0 , 10 , and 20 °C and 2 m/s), respectively.

Bioactive Compounds and Antioxidant Activity Analyses

Ergosterol content (EC) and total polyphenol content (TPC) (mg of ergosterol or GAE/g d.m.) (Fig. 4), and the antioxidant activity (AA) according to FRAP, CUPRAC, and ABTS methods (mg TE/g d.m.) (Fig. 5) in dried mushroom samples at 5, 10, and 15 °C without (AIR) and with 20.5 kW/m^3 of acoustic assistance (AIR+US), are shown in Figs. 4 and 5.

No significant ($p \geq 0.05$) differences were observed between EC of samples dried at 5 and 10 °C without ultrasound application (AIR) but significantly lower ($p < 0.05$) EC was observed in samples dried at 15 °C compared with samples dried at 5 °C. However, regarding TPC, no significant differences ($p \geq 0.05$) among dried samples at 5, 10, and 15 °C without ultrasound application (AIR) were observed. Comparing AA of dried samples without ultrasound application (AIR), significantly lower ($p < 0.05$) AA according to FRAP and CUPRAC methods were observed at 15 °C compared with dried sample at

5 °C but no significantly different ($p \geq 0.05$) AA in ABTS method were observed between them. Similar results were observed by Santacatalina et al. (2014) when drying apple at 5, 10, and 15 °C and 2 m/s. According to Santacatalina et al. (2014) TPC, total flavonoid content and AA according to CUPRAC and DPPH methods of dried samples at 0, 5, and 10 °C presented significantly lower ($p < 0.05$) figures with the increase of the temperature, meanwhile AA according to FRAP and ABTS methods presented no significant differences ($p \geq 0.05$) among those samples.

Considering dried samples at 5, 10, and 15 °C without (AIR) and with (AIR+US) ultrasound application, significantly higher ($p < 0.05$) EC and TPC figures were observed when ultrasound was applied during drying at each temperature. The increments were between 24 and 27% in EC and between 15 and 41% in TPC, compared with corresponding sample without ultrasound application, being higher as the temperature increased. AA figures according to all methods were not significantly different ($p \geq 0.05$) between samples dried at 5 °C without (AIR) and with (AIR+US) ultrasound application. However, significantly higher ($p < 0.05$) AA figures according to all methods were observed when ultrasound application was

Fig. 3 Light microscope photographs of dried samples at 5, 10, and 15 °C without (AIR) and with 20.5 kW/m^3 and 22 kHz of ultrasound application (AIR+US). s, shrinkage; h, hollows; m, micro-channels

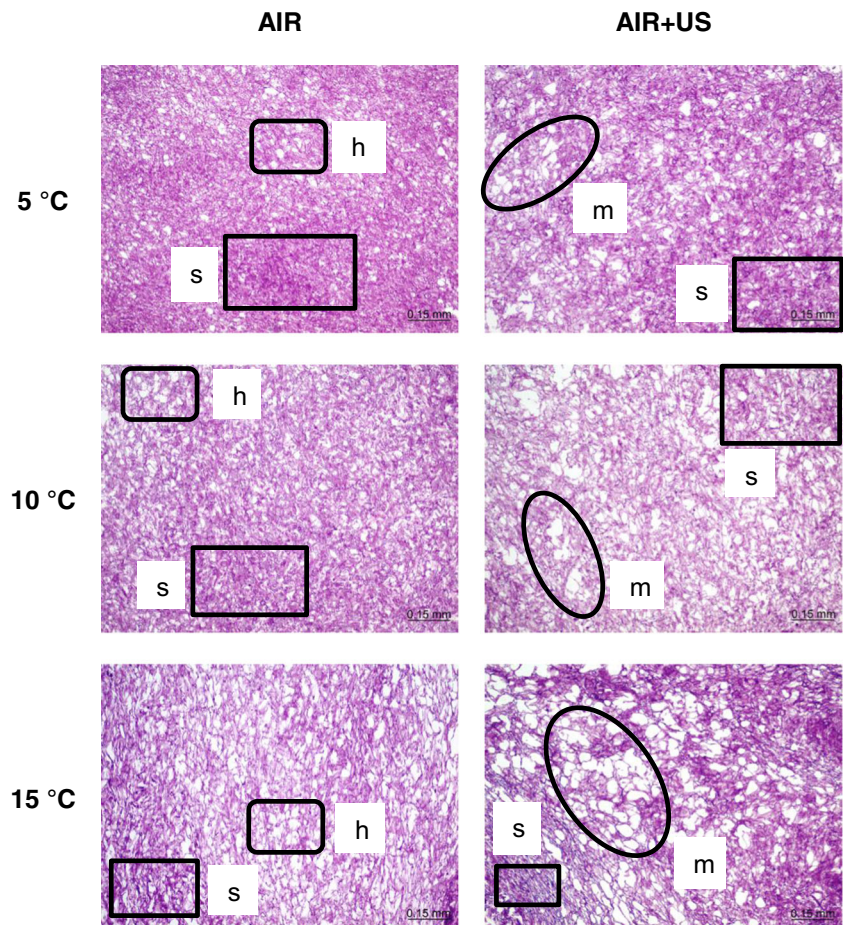
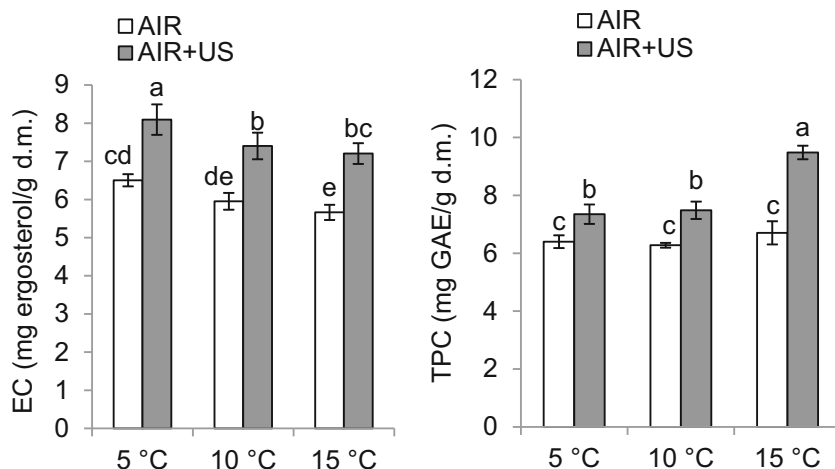


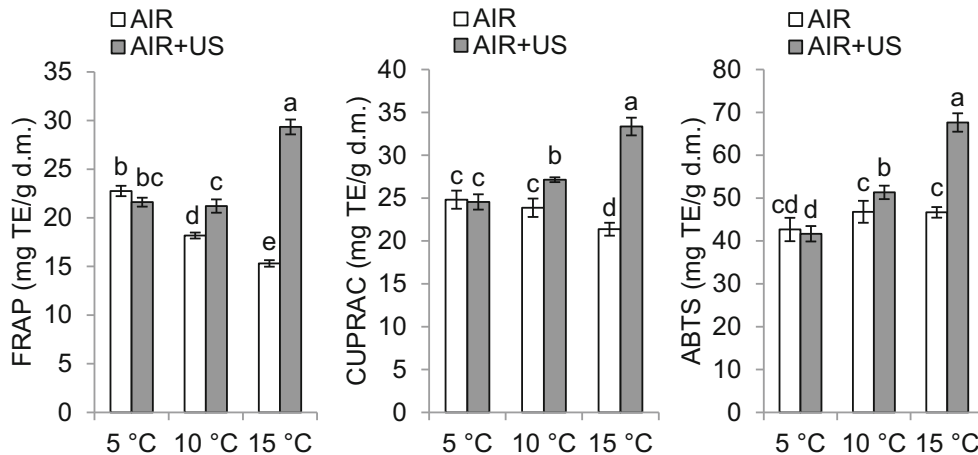
Fig. 4 Ergosterol content (EC) and total polyphenol contents (TPC) (mg of ergosterol or GAE/g d.m.) in dried mushroom samples at 5, 10, and 15 °C without (AIR, white bars) and with 20.5 kW/m³ and 22 kHz of acoustic assistance (AIR+US, gray bars). Average values ± standard deviations. Means with different letter for EC or TPC showed significant differences according to Tukey's test ($p < 0.05$)



carried out (AIR+US) at 10 and 15 °C compared with samples dried without ultrasound application (AIR). In this case, the increments ranged from 15 and 92% compared with the corresponding sample without ultrasound application, being also higher in samples dried at 15 °C than at 10 °C.

According to the results of Lagnika et al. (2013), ultrasound bath treatment (400 W during 10 min) on mushroom has been reported to maintain the TPC. Comparing with low-temperature drying of other products, since no bibliography about mushroom low-temperature drying was found, higher figures of TPC were also observed by Moreno et al. (2017) when ultrasound was applied (30.8 kW/m³) in apple slabs drying (at -10 °C and 2 m/s). Moreover, no significantly different ($p \geq 0.05$) AA figures according to FRAP and DPPH between apple-dried samples (at 5, 10, and 15 °C and 2 m/s) without and with ultrasound application (20.5 kW/m³) were reported by Santacatalina et al. (2014). Santacatalina et al. (2016a) reported also no significant differences ($p \geq 0.05$) in TPC and AA according to FRAP between apple-dried samples (at -10 and 10 °C and 2 m/s) without and with ultrasound application (20.5 kW/m³).

Fig. 5 Antioxidant activity (AA) according to FRAP, CUPRAC, and ABTS methods (mg TE/g d.m.) in dried mushroom samples at 5, 10, and 15 °C without (AIR, white bars) and with 20.5 kW/m³ and 22 kHz of acoustic assistance (AIR+US, gray bars). Average values ± standard deviations. Means with different letter for AA, according to FRAP, CUPRAC, or ABTS methods, showed significant differences according to Tukey's test ($p < 0.05$)



Color Determinations

Figure 6 presents the browning index (BI) figures of dried mushroom samples at 5, 10, and 15 °C without (AIR) and with 20.5 kW/m³ of ultrasound application (AIR+US). In average, dried samples without ultrasound application (AIR) presented a BI between 27 and 36 units which was close to the range of those reported by Nölle et al. (2017) in hot-air convective drying of mushroom at 40, 60, and 80 °C and 0.6 m/s (BI between 23 and 39 units). It can be observed that samples dried at 10 and 15 °C (AIR) presented significantly higher ($p < 0.05$) BI values than samples dried at 5 °C (AIR). Thereby, the increment of temperature from 5 to 10 °C promoted higher color coordinates changes and, consequently, higher BI figures. Also, significantly higher ($p < 0.05$) BI figures with higher temperatures were observed by Nölle et al. (2017) in hot-air convective drying of mushroom at 40, 60, and 80 °C and 0.6 m/s (23, 27, and 39 units, respectively).

The samples dried with ultrasound application (AIR+US) at 10 and 15 °C presented significantly lower ($p < 0.05$) BI than corresponding dried samples without ultrasound application (AIR). Significantly lower ($p < 0.05$) BI was also

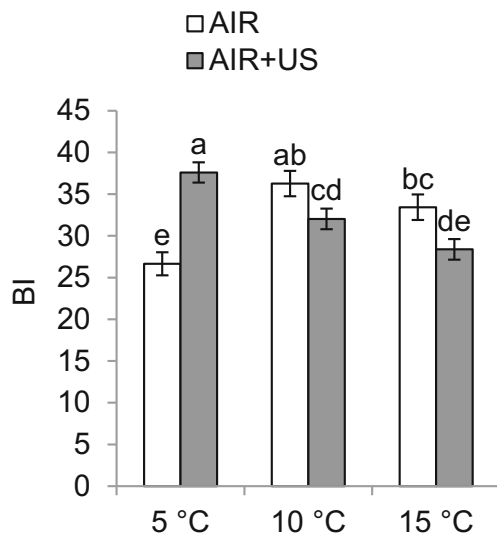


Fig. 6 Browning index (BI) of dried mushroom samples at 5, 10, and 15 °C without (AIR, white bars) and with 20.5 kW/m³ and 22 kHz of ultrasound application (AIR+US, gray bars). Average values \pm standard deviations. Means with different letter for BI showed significant differences according to Tukey's test ($p < 0.05$)

observed by Çakmak et al. (2016) in dried mushroom samples at 50 °C and 1.5 m/s with ultrasound bath pre-treatment at 450 W during 30 min (BI of 30.72 ± 0.06) compared with dried sample without pre-treatment (BI of 36.89 ± 0.12). However, BI of dried sample at 5 °C with ultrasound application (AIR+US) was significantly higher ($p < 0.05$) than the corresponding dried sample without ultrasound application (AIR), probably due to a longer ultrasound “sponge effect” exposure.

Hydration Properties and Fat Adsorption Capacity

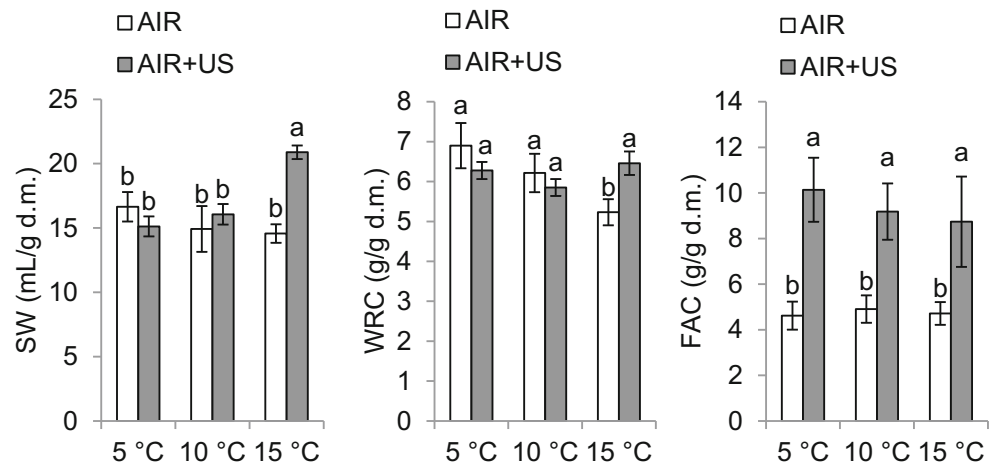
Figure 7 shows swelling (SW), water retention capacity (WRC), and fat adsorption capacity (FAC) of sieved powder (90–180 μ m) of mushroom samples dried at 5, 10, and 15 °C without

(AIR) and with 20.5 kW/m³ of ultrasound application (AIR+US). No references about hydration properties and fat adsorption capacity of dried mushroom were found. Therefore, comparisons with other dried products were carried out. SW and WRC values of mushroom samples dried without ultrasound application (AIR) were of 14.6–16.6 mL/g and 5.2–6.9 g/g, respectively, which were in the range of those reported by Femenia et al. (1997) for dried cauliflower florets and upper stems at 40 and 75 °C (4.2–17.5 mL/g and 5.7–18.2 g/g). FAC values of samples dried without ultrasound application (AIR) were of 4.6–4.9 g/g and they were in the range of the values reported by Femenia et al. (2009) in kiwi dried at 30 to 90 °C (4–10 g/g). In overall, compared with other fruits and vegetables, mushroom presented high hydration properties and fat adsorption capacity figures. In fact, Ekunseitan et al. (2017) observed significantly higher ($p < 0.05$) WRC and FAC in composite flour (wheat, cassava, and mushroom flour) when mushroom flour ratio was increased.

Samples dried at 5, 10, and 15 °C without ultrasound application (AIR) presented no significantly different ($p \geq 0.05$) SW and FAC. However, WRC values of samples dried at 5 and 15 °C without ultrasound application (AIR) were significantly different ($p < 0.05$). Thus, when ultrasound was not applied (AIR) lower WRC value was observed when the highest drying temperature was applied (15 °C). Similar results were observed by Garau et al. (2006) in WRC and FAC values of orange skin dried at 30–90 °C (particle size of 180 μ m). According to these authors, significantly lower ($p < 0.05$) WRC value was observed when increasing drying temperature and no significant differences ($p \geq 0.05$) in FAC values were observed when increasing drying temperature, excluding FAC value of sample dried at 90 °C which was significantly lower.

When ultrasound was applied (AIR+US), no significant differences ($p \geq 0.05$) in SW and WRC values were observed among dried samples at 5 and 10 °C without and with ultrasound application (AIR and AIR+US). However, sample dried at 15 °C with ultrasound application (AIR+US) presented significantly higher ($p < 0.05$) SW and WRC values than the corresponding

Fig. 7 Swelling (SW), water retention capacity (WRC), and fat adsorption capacity (FAC) of dried mushroom samples at 5, 10, and 15 °C without (AIR, white bars) and with 20.5 kW/m³ and 22 kHz of ultrasound application (AIR+US, gray bars). Average values \pm standard deviations. Means with different letter for SW, WRC, or FAC showed significant differences according to Tukey's test ($p < 0.05$)



sample dried without ultrasound application (AIR). With regard to FAC, all samples dried with ultrasound application (AIR+US) presented significantly higher ($p < 0.05$) values than corresponding samples without ultrasound application (AIR). Similar results were obtained also by Malik et al. (2017), thus, significantly higher ($p < 0.05$) FAC value was observed after ultrasound treatment of sunflower protein in bath (500 W and 40 kHz) or probe (500 W and 20 kHz) during 5, 10, 20, and 30 min, compared with sample without treatment.

Conclusions

When ultrasound was applied (AIR+US), significantly shorter ($p < 0.05$) drying times were observed (41–66% decrease) and significantly higher D_e (76–184% increase) and h_m (61–157% increase) coefficients were identified with the proposed diffusion model, compared with the drying without ultrasound application (AIR), within the studied temperature range (5–15 °C). Effects of ultrasound application were higher at higher drying temperature. Mushroom microstructure presented tissue shrinkage and hollows after drying at 5, 10, and 15 °C; meanwhile, ultrasound application during drying promoted micro-channels formation due to sponge effect, which were wider when increasing the temperature.

With regard to quality parameter changes when drying at different temperatures (5, 10, and 15 °C), significantly lower EC and AA (FRAP and CUPRAC), higher BI figures, and lower WRC value were observed when drying temperature increased up to 15 °C. However, when ultrasound was applied compared with experiments without ultrasound application (AIR), EC, TPC, and AA (all methods) figures were significantly higher or no significantly different at every temperature tested, significantly lower BI figures were observed at 10 and 15 °C and significantly higher hydration properties and fat adsorption capacity (SW, WRC, and FAC) values were obtained at 15 °C.

In brief, mushroom low-temperature drying process was intensified by using ultrasound application since mass transfer process was enhanced and, at the same time, quality parameters were preserved or improved comparing with drying process without ultrasound application, particularly when drying was carried out at 15 °C.

Funding Information The authors would like to acknowledge the financial support of the National Institute of Research and Agro-Food Technology (INIA) and co-financed with ERDF funds (RTA2015-00060-C04-03), the Balearic Government for the research project AAEE045/2017 co-financed with ERDF funds, and the Spanish Government (MINECO) for the BES-2013-064131 fellowship.

Nomenclature A, Face area (m²); BI, Browning index; D_e , Effective water diffusion coefficient (m²/s); D_o , Parameter in the effective diffusivity model (m²/s); E_a , Activation energy (kJ/mol); h_m , External mass transfer coefficient (kg water/m²s); L, Length (m); n, Number of experimental data; MRE, Mean relative error (%); R, Universal gas constant (J/mol·K); S_x , Standard deviation (sample); $S_{x,est}$, Standard deviation (estimation); T,

Temperature (°C); Th, Thickness (m); t, Time (h); V, Sample volume (m³); var, Percentage of explained variance (%); W, Average moisture content (kg/kg d.m.); x, Spatial coordinate (m); ρ_{dm} , Dry matter density (kg d.m./m³); φ , Relative humidity

Subscripts 0, initial; ∞ , drying air; cal, calculated; e, equilibrium at the surface; exp, experimental

References

- AOAC. (2006). *Moisture in dried fruits* (16th ed.). Maryland: Association of Analytical Communities.
- Çakmak, R. Ş., Tekeoğlu, O., Bozkır, H., Ergün, A. R., & Baysal, T. (2016). Effects of electrical and sonication pretreatments on the drying rate and quality of mushrooms. *LWT - Food Science and Technology*, 69(Supplement C), 197–202.
- Eim, V. S., Urrea, D., Rosselló, C., García-Pérez, J. V., Femenia, A., & Simal, S. (2013). Optimization of the drying process of carrot (*Daucus carota* v. Nantes) on the basis of quality criteria. *Drying Technology*, 31(8), 951–962.
- Ekunseitan, O. F., Obadina, A. O., Sobukola, O. P., Omemu, A. M., Adegunwa, M. O., Kajihausa, O. E., Adebowale, A.-R. A., Sanni, S. A., Sanni, L. O., & Keith, T. (2017). Nutritional composition, functional and pasting properties of wheat, mushroom, and high quality cassava composite flour. *Journal of Food Processing and Preservation*, 41(5), 1–8.
- Farokhian, F., Jafarpour, M., Goli, M., & Askari-Khorasgani, O. (2017). Quality preservation of air-dried sliced button mushroom (*Agaricus bisporus*) by lavender (*Lavendula angustifolia* mill.) essential oil. *Journal of Food Process Engineering*, 40(3), e12432.
- Femenia, A., Lefebvre, A. C., Thebaudin, J. Y., Robertson, J., & Bourgeois, C. M. (1997). Physical and sensory properties of model foods supplemented with cauliflower fiber. *Journal of Food Science*, 62(4), 635–639.
- Femenia, A., Sastre-Serrano, G., Simal, S., Garau, M. C., Eim, V. S., & Rosselló, C. (2009). Effects of air-drying temperature on the cell walls of kiwifruit processed at different stages of ripening. *LWT - Food Science and Technology*, 42(1), 106–112.
- Gamboa-Santos, J., Montilla, A., Cárcel, J. A., Villamiel, M., & Garcia-Perez, J. V. (2014). Air-borne ultrasound application in the convective drying of strawberry. *Journal of Food Engineering*, 128, 132–139.
- Garau, M. C., Simal, S., Femenia, A., & Rosselló, C. (2006). Drying of orange skin: drying kinetics modelling and functional properties. *Journal of Food Engineering*, 75(2), 288–295.
- García-Pérez, J. V., Ozuna, C., Ortuño, C., Cárcel, J. A., & Mulet, A. (2011). Modeling ultrasonically assisted convective drying of eggplant. *Drying Technology*, 29(13), 1499–1509.
- García-Pérez, J. V., Cárcel, J. A., Riera, E., Rosselló, C., & Mulet, A. (2012a). Intensification of low-temperature drying by using ultrasound. *Drying Technology*, 30(11–12), 1199–1208.
- García-Pérez, J. V., Ortuño, C., Puig, A., Cárcel, J. A., & Perez-Munuera, I. (2012b). Enhancement of water transport and microstructural changes induced by high-intensity ultrasound application on orange peel drying. *Food and Bioprocess Technology*, 5(6), 2256–2265.
- Giri, S. K., & Prasad, S. (2007). Drying kinetics and rehydration characteristics of microwave-vacuum and convective hot-air dried mushrooms. *Journal of Food Engineering*, 78(2), 512–521.
- González-Centeno, M. R., Jourdes, M., Femenia, A., Simal, S., Rosselló, C., & Teissedre, P.-L. (2012). Proanthocyanidin composition and antioxidant potential of the stem winemaking byproducts from 10 different grape varieties (*Vitis vinifera* L.). *Journal of Agricultural and Food Chemistry*, 60(48), 11850–11858.
- Guan, W., Zhang, J., Yan, R., Shao, S., Zhou, T., Lei, J., & Wang, Z. (2016). Effects of UV-C treatment and cold storage on ergosterol

- and vitamin D2 contents in different parts of white and brown mushroom (*Agaricus bisporus*). *Food Chemistry*, 210(Supplement C), 129–134.
- Heredia, J. B., & Cisneros-Zevallos, L. (2009). The effects of exogenous ethylene and methyl jasmonate on the accumulation of phenolic antioxidants in selected whole and wounded fresh produce. *Food Chemistry*, 115(4), 1500–1508.
- Iglesias, H. A., & Chirife, J. (1982). *Handbook of food isotherms: water sorption parameters for food and food components*. New York: Academic.
- Islam, M. N., Zhang, M., Adhikari, B., Xinfeng, C., & Xu, B.-G. (2014). The effect of ultrasound-assisted immersion freezing on selected physicochemical properties of mushrooms. *International Journal of Refrigeration*, 42(Supplement C), 121–133.
- Islam, M. N., Zhang, M., Fang, Z., & Sun, J. (2015). Direct contact ultrasound assisted freezing of mushroom (*Agaricus bisporus*): growth and size distribution of ice crystals. *International Journal of Refrigeration*, 57(Supplement C), 46–53.
- Lagnika, C., Zhang, M., & Mothibe, K. J. (2013). Effects of ultrasound and high pressure argon on physico-chemical properties of white mushrooms (*Agaricus bisporus*) during postharvest storage. *Postharvest Biology and Technology*, 82(Supplement C), 87–94.
- Lombraña, J. I., Rodríguez, R., & Ruiz, U. (2010). Microwave-drying of sliced mushroom. Analysis of temperature control and pressure. *Innovative Food Science & Emerging Technologies*, 11(4), 652–660.
- Malik, M. A., Sharma, H. K., & Saini, C. S. (2017). High intensity ultrasound treatment of protein isolate extracted from dephenolized sunflower meal: effect on physicochemical and functional properties. *Ultrasonics Sonochemistry*, 39(Supplement C), 511–519.
- Mihalcea, L. I., Bucur, F. C., Cantaragiu, A. M. M., Gurgu, L. C., Borda, D. D., & Iordachescu, G. S. (2016). Temperature influence on the *Agaricus bisporus* mushrooms dehydration process. *Scientific Study and Research: Chemistry and Chemical Engineering, Biotechnology, Food Industry*, 17(4), 323–333.
- Moreno, C., Brines, C., Mulet, A., Rosselló, C., & Cárcel, J. A. (2017). Antioxidant potential of atmospheric freeze-dried apples as affected by ultrasound application and sample surface. *Drying Technology*, 35(8), 957–968.
- Nöle, N., Argyropoulos, D., Müller, J. & Biesalski, H. K. (2017). Temperature stability of vitamin D2 and color changes during drying of UVB-treated mushrooms. *Drying Technology*, 36(3), 307–315. <https://doi.org/10.1080/07373937.2017.1326501>.
- Ozuna, C., Cárcel, J. A., Walde, P. M., & Garcia-Perez, J. V. (2014). Low-temperature drying of salted cod (*Gadus morhua*) assisted by high power ultrasound: Kinetics and physical properties. *Innovative Food Science & Emerging Technologies*, 23(Supplement C), 146–155.
- Paciulli, M., Ganino, T., Pellegrini, N., Rinaldi, M., Zaupa, M., Fabbri, A., & Chiavaro, E. (2015). Impact of the industrial freezing process on selected vegetables — Part I. Structure, texture and antioxidant capacity. *Food Research International*, 74, 329–337.
- Palacios, I., Lozano, M., Moro, C., D'Arrigo, M., Rostagno, M. A., Martínez, J. A., García-Lafuente, A., Guillamón, E., & Villares, A. (2011). Antioxidant properties of phenolic compounds occurring in edible mushrooms. *Food Chemistry*, 128(3), 674–678.
- Pei, F., Yang, W.-J., Shi, Y., Sun, Y., Mariga, A. M., Zhao, L.-Y., Fang, Y., Ma, N., An, X.-X., & Hu, Q.-H. (2014). Comparison of freeze-drying with three different combinations of drying methods and their influence on colour, texture, microstructure and nutrient retention of button mushroom (*Agaricus bisporus*) slices. *Food and Bioprocess Technology*, 7(3), 702–710.
- Reay, D., Ramshaw, C., & Harvey, A. (2013). *Process intensification: engineering for efficiency, sustainability and flexibility*. Amsterdam: Elsevier Science.
- Reis, F. S., Martins, A., Vasconcelos, M. H., Morales, P., & Ferreira, I. C. F. R. (2017). Functional foods based on extracts or compounds derived from mushrooms. *Trends in Food Science & Technology*, 66(Supplement C), 48–62.
- Rodríguez, Ó., Eim, V. S., Simal, S., Femenia, A., & Rosselló, C. (2013). Validation of a diffusion model using moisture profiles measured by means of TD-NMR in apples (*Malus domestica*). *Food and Bioprocess Technology*, 6(2), 542–552.
- Rodríguez, Ó., Santacatalina, J. V., Simal, S., Garcia-Perez, J. V., Femenia, A., & Rosselló, C. (2014). Influence of power ultrasound application on drying kinetics of apple and its antioxidant and microstructural properties. *Journal of Food Engineering*, 129, 21–29.
- Rodríguez, O., Eim, V., Rossello, C., Femenia, A., Carcel, J. A., & Simal, S. (2018). Application of power ultrasound on the convective drying of fruits and vegetables: effects on quality. *Journal of the Science of Food and Agriculture*, 98(5), 1660–1673.
- Salehi, F., Kashaninejad, M., & Jafarianlari, A. (2017). Drying kinetics and characteristics of combined infrared-vacuum drying of button mushroom slices. *Heat and Mass Transfer*, 53(5), 1751–1759.
- Santacatalina, J., Rodríguez, O., Simal, S., Cárcel, J., Mulet, A., & Garcia-Pérez, J. (2014). Ultrasonically enhanced low-temperature drying of apple: influence on drying kinetics and antioxidant potential. *Journal of Food Engineering*, 138, 35–44.
- Santacatalina, J. V., Contreras, M., Simal, S., Cárcel, J. A., & Garcia-Perez, J. V. (2016a). Impact of applied ultrasonic power on the low temperature drying of apple. *Ultrasonics Sonochemistry*, 28(Supplement C), 100–109.
- Santacatalina, J. V., Guerrero, M. E., Garcia-Perez, J. V., Mulet, A., & Cárcel, J. A. (2016b). Ultrasonically assisted low-temperature drying of desalted codfish. *LWT - Food Science and Technology*, 65(Supplement C), 444–450.
- Santacatalina, J. V., Soriano, J. R., Cárcel, J. A., & Garcia-Perez, J. V. (2016c). Influence of air velocity and temperature on ultrasonically assisted low temperature drying of eggplant. *Food and Bioprocess Technology*, 100(Part A), 282–291.
- Shao, S., Hernandez, M., Kramer, J. K. G., Rinker, D. L., & Tsao, R. (2010). Ergosterol profiles, fatty acid composition, and antioxidant activities of button mushrooms as affected by tissue part and developmental stage. *Journal of Agricultural and Food Chemistry*, 58(22), 11616–11625.
- Spanish Government. (2018). Fábrica Nacional de Moneda y Timbre-Real Casa de la Moneda. Available at <http://www.fnm.t.es/en/institucion/informacion-institucional>. Accessed 28/11/2018 2018.
- Urun, G. B., Yaman, Ü. R., & Köse, E. (2015). Determination of drying characteristics and quality properties of eggplant in different drying conditions. *Italian Journal of Food Science*, 27(4), 459–467.
- Vallespir, F., Rodriguez, O., Carcel, J. A., Rossello, C. & Simal, S. (2018). Ultrasound assisted low-temperature drying of kiwifruit: effects on drying kinetics, bioactive compounds and antioxidant activity. *Journal of the Science of Food Agriculture*. <https://doi.org/10.1002/jsfa.9503>.
- Wu, X., Guan, W., Yan, R., Lei, J., Xu, L., & Wang, Z. (2016). Effects of UV-C on antioxidant activity, total phenolics and main phenolic compounds of the melanin biosynthesis pathway in different tissues of button mushroom. *Postharvest Biology and Technology*, 118, 51–58.
- Zhang, Z., Liu, Z., Liu, C., Li, D., Jiang, N., & Liu, C. (2016). Effects of ultrasound pretreatment on drying kinetics and quality parameters of button mushroom slices. *Drying Technology*, 34(15), 1791–1800.